Supported By
tetfund
TERTIARY EDUCATION TRUST FUND

DEVELOPMENT OF AERATED AND MECHANICALLY AGITATED FROTH FLOTATION MACHINE

O.O. Ajibola[1*], A.O. Adebayo[1], S.G. Borisade[1], A.F. Abubakar[1], K.V. Oguntade[1], D.O. Omoyeni[2]
[1]Department of Materials and Metallurgical Engineering, Federal University Oye Ekiti
[2]Department of Mineral and Petroleum Resources Engineering, Federal Polytechnic, Ado Ekiti
*olawale.ajibola@fuoye.edu.ng, abdullahi.adebayo@fuoye.edu.ng, sunday.borisade@fuoye.edu.ng,
***Correspondence:** olawale.ajibola@fuoye.edu.ng

Received: December 13, 2021 Accepted: March 20, 2022

ABSTRACT The fabricated beneficiation system is based on the froth flotation principle whereby the mineral flotation is done by supply of air bubbles and rotating impeller in large mineral pulp bath. The mineral pulp to be separated is fed into the mixing chamber with the required flotation reagents, thoroughly mixed prior to its introduction into the flotation bath. The bath agitation is induced via the combination of installation of the electric motor powered impellers and the air from blower is introduced into the floatation bath. Mineral flotation process commences when the bubbles lift up the very light particles to the face of flotation bath after serious agitation and separated in form of froth. The machine design is centered on review works on the existing machines. The flotation cell was designed in simplicity based on scientific principles of froth flotation for efficient and economic minerals separation. On the laboratory scale, the cell is capable of separating about 15-25 kg mineral concentrates per day. The machine fabrication estimated cost is about ₦223,350:00.

Keywords: aeration; flotation cell; pulp; froth; concentrate; tailings, minerals, surfactants

INTRODUCTION

Water and solid waste pollutions are among of the most challenging problems in mining, mineral processing and metallurgical industries. In ore processing, flotation methods have been employed in alleviating many ecological challenges. Flotation offers a simple and cheap solutions to waste recycling and sewage treatment industries (Kaya, 2005, Michuad, 2016); pulp and paper, textile, food, plastic, petroleum, water purification, used in mineral processing for 10-200 μm fine particles (Kwatra, 2015); and chemical engineering for the separation and concentration of aqueous suspensions or solutions of a variety of precipitates, inorganic waste constituents, and even microorganisms and proteins.

For years, froth flotation is renowned for the isolating solids in the primary chemical and mineral beneficiation industries (Somasundaran and Kunjappu, 1989; Dibrov *et al.*, 1998, Nelson, 2012). Froth flotation technique is principled on the physico-chemical properties of surface such as wettability and surface charge of the components to be separated. The practice of selectively separates water repelling (hydrophobic) from the water attracting (hydrophilic) materials (Jameson, 2010a, 2010b). Adding flotation agents could significantly enhance the surface properties of mineral particles to increase the separation efficiency (Li *et al.*, 201; Aghazadeh *et al.*, 2015). Li *et al.*, (2019) reported high mineral recovery efficiency from flotation testing of hematite, quartz and apatite using surfactants under wide array of pH. Flotation is useful in beneficiating sulphides from silica gangue or other mineralized sulphides; extraction of KCl (sylvite) from NaCl (halite); coal from ash-forming minerals; eliminate mineralized silicates from iron ores; eradicating mineralized phosphates from silicates. It also applies to de-inking of non-mineral applications like recycled newsprint. It is particularly useful for processing fine-grained ores that are not amenable to conventional gravity concentration, iron and non-ferrous metals, non-metallic minerals and coal (Kwatra, 1987; Smieszek, 2001).

The gravity and dense medium separation DMS processes renowned for beneficiating coarse coal (+500 μm) particles, while the froth flotation is mostly proficient process for cleaning fine coal (−500 μm) particles (Laskowski, 2001) and separation columns are superior to conventional mechanical cells in cleaning fine coal (Rubinstein, 1995; Yoon *et al.*, 1992; Eberts, 1986). Oscillatory air generator with fast-switching solenoid valve was reported by Li and Wang, (2018) for column flotation of fine silica particles. The test was uninterruptedly performed using a customised column to win silica from the froth zone.

Of numerous number of flotation equipment available, mechanical or conventional cells, energy-intensive pneumatic cells, column cells (Degner, 1988) and froth separators, the mechanical floatation cell dominated the mineral industries since the early days

and accounted for a significant amount of mineral processed. The impeller stirs and diffuses air into the pulp. The impeller fitted in the mechanically controlled flotation tanks performs major function in sustaining minerals in suspension, dispersion and splitting air bubbles, and allowing collision of mineral-bubble. Nonetheless, the impeller generated turbulent regime which affect the pulp-froth interface and the overall separation result (Allen, 1995; Deglon, 2005; Tabosa *et al.,* 2016; Mesa and Brito-Parada, 2019). Mesa *et al.,* (2020) investigated two designs of impellers with and without a stator on the result of laboratory-scale outsized flotation tank (array of air flow rates, pulp bubble size, froth stability and mineral recovery).

The coal flotation circuits are designed based on kinetics results derived from laboratory scale batch flotation which usually differs from the plant flotation results. The combined facts imply that diverse machine sizes and designs can give comparable flotation performance when the working variables are properly moderated (Taggart, 1945; Harris and Lepetic, 1966; Arbiter and Harris, 1979; Xia *et al.*, 2016). The impact of bath volume and impeller agitation speed on performance of batch coal flotation in a self-aerating machine was investigated by Anzoom *et al.,* (2020) via experimental factorial design to ascertain the correlation among the influencing factors (agitation speed, cell volume, and their relations) with the concentration indicators (entrained water recovery, ash, combustible recovery and the yield).

In the NovaCell fluidized bed froth flotation column, coarse particles settle at the base of a column and are fluidized by an upward-flowing stream of liquid. Introduced air bubbles with the flow have collision with particles of water-repelling minerals on the bed and transmit them as froth to the uppermost level of the container. In the development of new flotation equipments, Jameson, 2010a, 2010b described an innovative froth flotation device with fluidized state coarse particles bed, maintained by a circulating stream with integration of a bubble contactor. Recently, Jameson *et al.,* (2020) described using clusters (floating bubble and mineral particle collections) as solution to recover valuable minerals during flotation.

However, innovative flotation devices, monitoring, measurement and analytical methods were developed, introduced and in use (Gorain, 2000). Improvement in control and maximisation of froth flotation practice are of immense significance because very small rise in recovery lead to huge economic profits (Ferreira and Loveday, 2000; Maldonado *et al.,* 2007a,b). Quintanilla *et al.,* (2021 suggested that employing advanced controller that is very reliant on the model centered on the dynamics of the process (such as Model Predictive Control, MPC) as one outstanding way to enhance flotation performance. Applying machine vision system (MVS) gained significant advancements in automation of froth flotation procedure in past years. Aldrich *et al.,* 2010 review report established that machine vision is able to accurately and rapidly extract froth characteristics. Both the physical (such as bubble dimension) and the dynamics (velocity of froth) obtained from digital images results are use as procedural inputs to control systems.

These days, on-streamX-ray analyzers are incorporated in the flotation process plants for continuous quantification of the key streams and estimation of performance. However, high capital and maintenance costs are the shortcomings of these devices (Holtham and Nguyen, 2002). The real time process monitoring and control in flotation is not straight forward because of a vast factors involved (Bergh and Yianatos, 2011; Jovanovic and Miljanovic, 2015; Jovanovic *et al.,* 2015; Saravani *et al.,* 2014; Shean and Cilliers, 2011). In the Jahedsaravani's *et al.*, (2017) used the MVS in extracting the visual traits from the froth images and the obtained results were presented to the control systems. In another case, Zarie *et al.,* (2020) developed a complex neural network (CNN) to categorize the coal froth images obtained from flotation column in diverse practice circumstances (air flow rate, pulp solids%, collector and frother dosages, etc) from which the overall results of 93.1% accuracy was obtained. The on-line plant installation had recorded several successes for years along which Kaartinen *et al.,* (2009) used generic, modular and scalable MVS for single or multiple camera for rapid-prototyping applications.

In designing a froth flotation cell, some important and interrelated parameters and components put into consideration include: the surface chemistry (pH, frothers, depressants, activators, collectors); equipment components (agitation air flow, flotation cell design, cell tank shape, control operation); materials feed rate, mineralogy, pulp density, temperature (Schulze, 2004). Altering the settings any factor (mineral feed rate) definitely changes order of the system (like air flow, flotation rate, pulp density and recovery, etc,). Thus, it is not easy to study the consequence of any single factor in isolation, and compensation effects can keep system from producing the expected results (Bergh and Yianatos, 2011; Saravani *et al.,* 2014). This makes it not easy to produce models to forecast froth flotation behaviour, although there are simple models for predicting the outcome of the scheme from parameters: recovery of minerals and tailings solid content (Kawatra, 2015; Rao *et al.,* 1995).

Entrainment refers to getting hydrophilic minerals in form of froth alongside with the water (Warren, 1985; Trahar, 1981). Investigations on the batch flotation by Angadi *et al.,* (2012) assessed the kinetics of water streams and mineral froths. The functions of diverse factors on minerals and water flow are obtained anchored on the tests on column flotation and usual (batch) cells using fine particles of coke.

The quantitative measure of froth dwelling time is vital diagnostic instrument in design and managing of flotation cells and in evaluating froth mineral recovery (Mathe *et al.,* (2000). Yianatos *et al.,* (2008) evaluated the froth average residence times by directly measuring time responses of liquid solution and mineral in the copper filled froth of self-aerated flotation cells.

It was alleged that froth rheology affects froth and flotation act base on information on experimental work done using synthetic ore consisting of mixture of silica and pure chalcopyrite (Li *et al.,* 2018).

Froth stability powerfully controls the separation, as much that it is linked with the mineral particle size, mineral content and the quality of water. Liu et al., (2020) studied froth stability and froth drainage by reverse flotation using cellophane with cationic surfactant.

Nunez *et al.,* (2009) demonstrated using step response analysis, that froth speed is closely related to pulp level; and proposed a piecewise affine structure for froth speed-pulp level relation, yielding a hybrid model obtained applying hybrid detection method to actual industrial statistics from flotation line.

A mechanical floatation cell essentially consists of a vessel or a tank rotated with an impeller or rotor. The impeller stirs up the pulp to preserve the minerals in suspension, scatters air into fine bubbles; and gives room for contact of bubbles and hydrophobic minerals; attachment and separation of valuable minerals from the unwanted gangues in the flotation tank. The bubble particles unite rise up by buoyancy in the flotation cell and are isolated from the cell edge into the inclined launder (collection box) as product known as concentrate. However, the detached mineral particles (hydrophilic minerals) are released through the bottom of the flotation tanks to tailings box (Gorain, 2000).

Flotation cells are needed in the cottage mineral processing industries and sand treatment unit of foundries, therefore the need to develop a low cost, functional flotation cell using locally sourced materials at a relative low cost and environmental safety. The main target of the present work is to design and fabricate a simple sub aeration flotation cell suitable for separation of unwanted wastes from the valuable minerals.

MATERIALS AND METHODS

Conceptualization

The process of design is long and time consuming. A new or better machine and its component should be more economical in the overall cost of production and simpler to operate. Knowing and deciding the shapes of individual component of machine is a fundamental part of design process. It represents the truly creative stage, the creation of a mechanism or structure in the mind etc. using intuition, thought and imagination. The designer tries the best possible concept without initially giving thought to relationship of individual dimension, perhaps with no particular scale in mind. Materials selection of component parts of the machine was factored on good durability consideration, nature of the operation, corrosion resistance, ease of production, availability, cost and aestheticism. For the aggressiveness of flotation chemicals, angle steel bar of 50 mm thickness was used for the construction of the frame and stainless steel metal plate of 1.5mm was adopted for the mixing chamber and floatation bath. The design process requires good knowledge of fundamental courses in Science and Engineering such as mathematics, engineering drawing, strength of material, fluid mechanics, hydrodynamics, thermodynamics surface chemistry, electrostatics, and theory of machine and workshop practices.

Design calculations

The design of the components of the machine is based on the fundamental scientific principles and theories which are expressed by the following mathematical equations:

Power Requirement

The design in its current state is low energy consumption; comprising both 0.5 Hp electrical energy driven motor with shafts, pulleys and belts driven impeller.

Power drive design

The electrical energy driven motor drives the 3 shafts, 4 pulleys, 2 belts and 2 impellers. Each of the long mixing shafts is connected to 2 sets of pillow bearings to maintain the stability during rotation of the shafts. The power was determined from equations (1) and (2);

$$P = \frac{\text{workdone}}{\text{time}} = \frac{(\text{force x distance})}{\text{time taken}} \quad (1)$$

$$\text{Total work done} = (W_R + W_P) \times d \quad (2)$$

Where : W_R is Work done on shaft rod weight with impeller, W_P is Work done on pulp (i.e mineral + water), d is height of the rod

Prime motor speed

The required Motor Speed **and** power rating (Hp) were determined from equations (3) and (4);

$$\text{Motor Speed (rpm)} = \frac{120 * \text{ frequency}}{\text{no of poles}} \quad (3)$$

$$\text{Motor power rating (HP)} = \frac{\text{Torques} * \text{ rpm}}{5250} \quad (4)$$

Considerations for shafts, pulleys and belts design

The parameters for the shafts, pulleys and belts belt length were determined according to Equations (5) to (19) adapted from Dairo *et al.*, (2017), Erameh and Adingwupu, (2019), Ajibola (2020). To determine the moment of inertias; X1 to X13 connotes the distances among the components in figure 1 (b).

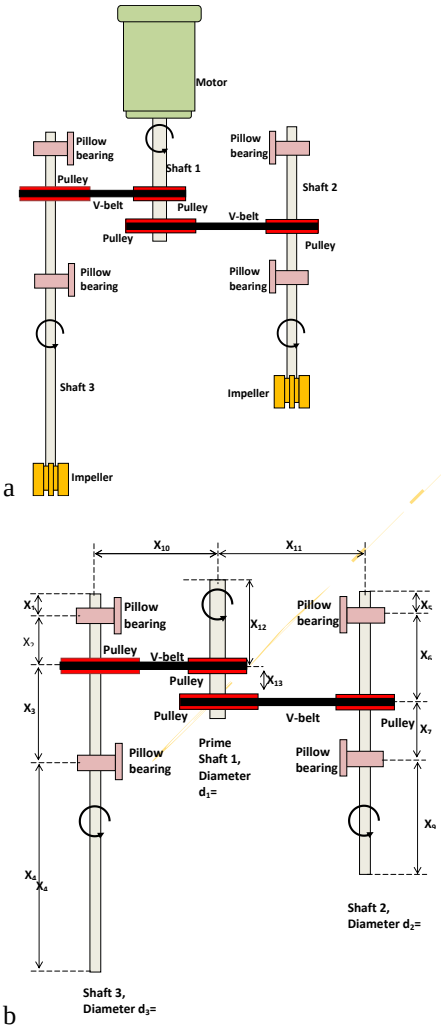

Figure 1: Energy transmission and torque by shafts, pulleys, pillow bearings and belts assembly

Torsion and torque calculation

$$\text{Torque (Nm)} = \frac{HP * \ 5250}{rpm} \quad (5)$$

Torque Transmission

The shaft radii under torsional forces are determined from mathematical expressions in (6) to (8)

$$\tau = 2T/\pi(r)^3 \quad (6)$$

Thus, $$r = 0.5\left(\sqrt[3]{\frac{5.1T}{\tau}}\right) \quad (7)$$

$$d = 2r \quad (8)$$

where $\boldsymbol{\tau}$ is torsion, $\boldsymbol{T}$ is torque, r is the radius and $\boldsymbol{d}$ is shaft diameter (Dairo *et al.*, 2017).

Accordingly, for a line shaft carrying pulleys, the torque on the shaft is presented by Erik *et al*, (2004) as equation (9):

$$T_s = (9.55\text{x } 10^6 \text{ P})/\text{N} \quad (9)$$

where $\boldsymbol{T_s}$ is torque on the shaft, $\boldsymbol{P}$ is power input, $\boldsymbol{N}$ is rotational speed of the shaft.

Angular velocity ω, at certain speed is given by (10):

$$\omega = \left(\frac{2\pi N}{60}\right) \quad (10)$$

The angular velocity, $\boldsymbol{\omega}$ of the motor and transmitted power $\boldsymbol{H}$ (in kwh) through the shafts, pulleys and belts are calculated using (11) and (12) (Erameh and Adingwupu, 2019):

$$H = M_t\omega_t \quad (11)$$

$$M_t = \frac{30H}{\pi N} \quad (12)$$

where $\boldsymbol{M}$ is bending moment at the point of interest

In case of the shaft design based on Strength, the stress at any point depends on the nature of load acting on the shaft presented as basic stress equations (13)-(19) for shaft design (Khurmi and Gupta, 2005) as follows:

The bending stress is defined as;

$$\sigma_b = \frac{32M}{\pi d_0^3(1-k^{-4})} \quad (13)$$

where, $\boldsymbol{M}$ is the bending moment at the point of interest, $\boldsymbol{d_o}$ is the outer diameter of the shaft, $\boldsymbol{k}$ is the ratio of inner to outer diameters of the shaft (in the present case, k = 0 for a solid shaft since the inner diameter is zero)

The Axial stress is defined in (14) as;

$$\sigma_s = \frac{4\alpha F}{\pi d_0^3(1-k^{-4})} \quad (14)$$

where, ***F*** is Axial force (tensile or compressive), ***α*** = column-action factor (1.0 for tensile load). α is called column action factor, due to buckling of long slender parts subjected to axial compressive loadings and it is defined as (15) and (16);

$$\alpha = \frac{1}{1-0.0044(L/K)} \quad \text{For L/K <115} \quad (15)$$

$$\alpha = \frac{\sigma_{yc}}{\pi^2 nE}\left(\frac{L}{K}\right)^2 \quad \text{For L/K >115} \quad (16)$$

n = 1.0 for hinged end, n = 2.25 for fixed end, n = 1.6 for ends partly restrained, as in bearing, ***K*** is the least radius of gyration, ***L*** is the shaft length, σ_{yc} is the yield stress in compression

The torsional stress is given by (17)

$$\tau_{xy} = \frac{16T}{\pi d_0^3(1-k^{-4})} \quad (17)$$

T is the torque on the shaft, and τ_{xy} is the shear stress due to torsion

The bending and axial stresses are normal stresses represented by equation (18);

$$\sigma_b = \left[\frac{32M}{\pi d_0^3(1-k^4)} \pm \frac{4\alpha F}{\pi d_0^2(1-k^2)}\right] \quad (18)$$

Shear stress due to torsion is only considered in a shaft and shear stress due to neglected load on the shaft.

The maximum shear stress theory as related to the shaft design is given as (19);

$$\tau_{max} = \tau_{allowable} = \sqrt{\left[\frac{\sigma_x}{2}\right]^2 + \tau_{xy}^2} \quad (19)$$

Pulley and belt parameters

Following Erik *et al*, (2004); the pulley diameters are determined from (20):

$$\text{Pulley Diameter, } d_p = (1200 \sim 150)\sqrt[3]{\frac{P}{n}} \quad D = id \quad (20)$$

where P = pitch diameter, n = revolution of given pulley, d_p = pulley diameter, i = required belt speed.

Based on the illustration in Figure 2, the belt lengths are determined from (21):

$$\text{Belt length, } BL = 2c + \frac{\pi}{2}(d + D) + \frac{(D-d)^2}{4c} \quad (21)$$

where, c = center length between two pulleys, d = distance of small pulley, D = distance if large pulley, L = belt length

For the rotating shaft-pulley connection; the following design parameters are calculated considering the equation (22) by Khurmi and Gupta, (2005):

$$\frac{D_S}{D_D} = \frac{N_D}{N_S} \quad (22)$$

where D_S is diameter of pulley connected to the spiral shaft, D_D is diameter of pulley on power drive, N_D is the speed of power drive and N_S is the speed of spiral agitator.

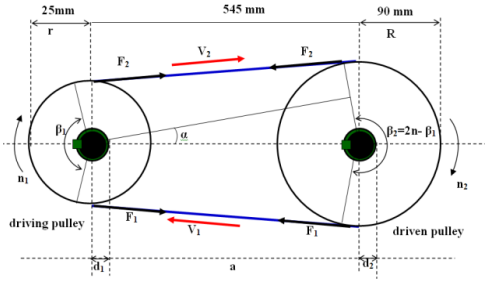

Figure 2: belt and pulleys transmit motion and torque through the shafs (Ajibola *et al*., 2020)

Pulp mixer design

The volumetric capacity and efficiency of the mixer parameters for the mixing chamber are determined from equations (23) to (25);

Volumetric capacity of mixing chamber

Volume of mixing chamber (V_{mc}) = Cylindrical Part (V_1) + Conical Part (V_2)

$$V_{mc} = (V_1) + (V_2) \quad (23)$$

For cylindrical part, $\boldsymbol{V_1} = \pi r^2 h$ (23.1)

where ***r*** is radius of the cylinder, ***h*** is height of cylinder and π = 3.143

For conical part, $\boldsymbol{V_2} = \frac{1}{3}\pi r^2 h$ (23.2)

where ***r*** is radius of the cone, ***h*** is height of the cone

Efficiency of the mixer was determined using equations (24) and (25) according to Osarenmwinda and Iguodala, (2014);

Efficiency of the mixer ***ε***,

$$\varepsilon = \frac{\text{Output power}}{\text{Input power}} \text{ x } 100\% \quad (24)$$

For the homogenizer, the efficiency is determined by

$$\varepsilon = \frac{\text{Power required}}{\text{Power supplied}} \text{ x } 100\% \quad (25)$$

Flotation cells design

The flotation cell design is complex, comprising the configurations of the baths, impeller design, air generator design, fluid flow properties, pulp-reagents

characteristics and other factors. These parameters are inter-related and were resolved using diverse mathematical expressions (26) to (36).

Volumetric capacity of the flotation bath

Volume of each of the flotation bath is determined as (26);

$$V_{bath} = (l \times b \times w)_{bath} \quad (26)$$

l is length of flotation bath, ***b*** = breath of flotation bath, ***w*** = width of flotation bath.

Radial flow mixing impellers design

As in the present case, typical radial flow impellers commonly used in dispersion of particles in liquid applications are adapted for mixing mineral pulp (in mixing tank) and pulp agitation (in flotation cell) as illustrated in Figure 3. The features involved are centred mostly some design parameters such as: impeller horsepower, motor horsepower, primary flow, bulk velocity, shafts design parameters (hydraulic side force, torsion and bending and critical speed) and Reynolds number. By a general rule, for both axial and radial flow, the impeller diameter is recommended as one-third of vessel diameter. The parameters for the Impeller and configurations were determined according to equations (27) to (37) (Crane Engineering Manual)

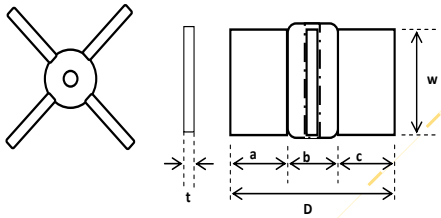

Figure 3: 2D of plan and side views of the radial type 4 blade impeller

D = a + b + c; a = c

where, D = impeller diameter, w = blade width, t = blade thickness

Reynolds Number

N_{Re} is a dimensionless number that characterizes the fluid regime at the impeller. It is the ratio of inertial forces to viscous forces, and links Power Number (N_P) and Pumping Number (N_Q) parameters for impellers.

$$\textbf{Reynolds Number} \quad N_{Re} = \frac{10.7 S_g N D^2}{\mu} \quad (27)$$

N_{Re} is Reynolds number, S_g is specific gravity of fluid, N is rotational speed (rpm), D is impeller diameter, μ is fluid viscosity.

Impeller Horsepower

For a mixing application in water with fully baffled tanks, the power requirement is primarily a function of the impeller design (N_P), the operating speed (N), the impeller diameter (D) and the fluid specific gravity (S_g).

Impeller Horsepower rating

$$P = \frac{N_p N^3 D^5 S_g}{1.52(10^{13})} \quad (28)$$

P is impeller horsepower, N_P is impeller power number (corrected for proximity & Reynolds number), N is rotational speed (rpm), D is impeller diameter and S_g is fluid specific gravity

Motor Horsepower

For a given mixing impeller to operate at the design speed under design conditions; the motor horsepower must be adequate and in addition, the reducer losses were accounted for.

$$\textbf{Motor horsepower} \quad Hp = \frac{P}{(Eff)(\%Ld)} \quad (29)$$

Hp is motor horsepower, P is impeller horsepower, ***Eff*** is reducer efficiency, and % Ld is motor loading (90% max.)

Primary Flow

Primary flow or the impeller displacement is important in impeller calculation and it is also dependent on both the operating speed (N) and impeller diameter (D) as shown:

$$\textbf{Primary flow} \quad Q_p = \frac{N_Q N D^3}{231} \quad (30)$$

Q_P is Primary flow (g/m), N_Q is pumping number, N is rotational speed (rpm) and D is impeller diameter.

Bulk Velocity

Bulk velocity measures the relative agitation and defined as unit of flow per unit of vessel cross-sectional area.

$$\textbf{Bulk velocity} \quad V_B = \frac{Q_p}{7.48\,A} \quad (31)$$

V_B = bulk velocity, Q_p = primary flow (g/m), A = cross sectional area of tank

Impeller shafts design parameters

The design accounts for unwanted feature that commonly affects the auxiliary equipment such as the shaft, reducer, seal and the support structure in center mounted agitators in fully baffled tanks:

$$\textbf{Hydraulic Side Force } F = KN^{1.67} D^{3.53} S_g \quad (32)$$

where K is constant (geometry factor), N is rotational speed (rpm), D is impeller diameter, S_g = fluid specific gravity

The values of K (Table 1) and the powers of N and D have been empirically determined for various conditions as shown

.

Table 1: The values of K

	Non-Vortex	Vortex
Typical 4-blade axial flow turbine	0.0005	0.0025
Typical 4-blade radial flow turbine	0.0010	0.0050

Torsion and Bending

Equation (33) is used to calculate the required diameter size of power transmission shaft as a function of the combined loading (torsion and bending) and the allowable stress.

Shaft diameter $d^3 = \frac{16}{\pi S_s}\sqrt{(FL)^2 + (\tau)^2}$ (33)

d is minimum shaft diameter, S_s is allowable shear stress, F is hydraulic side force, L is shaft length, and τ is torque

As in the present design, to calculate the shaft critical speed of a single stepped shaft for solid or hollow shafts whereby all weights of impellers, couplings, etc. are transferred to the end of the shaft by the equivalent weight equations in *(34) and (35).*

Equivalent Weight,

$$W_e = W_1 + W_2\left(\frac{L_2}{L_1}\right)^3 \dots\dots \quad (34)$$

Critical Speed Calculation,

$$N_{C_1} = 146\frac{d_A^2}{L}\sqrt{\frac{E}{\left[(L+a)L+\frac{(RS-1)C^3}{L}\right]\left[4.13\frac{We}{L}+W_B\right]}} \quad (35)$$

N_{C_1} = first shaft critical speed (rpm), d_A = upper shaft outside diameter, L = shaft length (bearing to C impeller), E = modulus of elasticity, a = bearing span, R = I_A / I_B (where A is upper shaft moment of intertia and B is lower shaft moment of intertia), S = weight factor (S = 1 for 316 and 304 stainless steel, Carbon steel), C = lower shaft length (C > 0.75L), W_e = equivalent weight, W_B = weight/cm of lower shaft

Air generator design

The selection of the air pump/blower power rating or capacity is based on Equation (36)

Blower power rating (HP) = $\frac{Volume * Pressure)}{3300 * Mech\ Eff\ of\ blower\ fan}$ (36)

Flotation Rate

The flotation rate is determined from the common equation that describes the recovery of the particle with respect to the flotation kinetics as given as (37);

$$R = R_{max}\left[1 - \frac{1}{kt}(1 - e^{-kt})\right] \quad (37)$$

where ***R*** is recovery of particles in the final product, ***K*** is flotation rate constant

t is flotation time, $\boldsymbol{R_{max}}$ is ultimate/ maximum recovery of the particle in the froth product

Flotation efficiency calculations

The collection efficiency of a froth flotation process is found from the *flotation recovery* (R) equation (38) which links the probabilities of collision and attachment of particles to air flotation bubbles (wiki/Froth_flotation, Froth Flotation, 2019).

$$\boldsymbol{R} = \frac{\boldsymbol{N_c}}{\left(\frac{\pi}{4}\right)(\boldsymbol{d_p} + \boldsymbol{d_b})2\,\boldsymbol{Hc}} \quad (38)$$ (wiki/Froth_flotation)

where: $\boldsymbol{Nc} = \boldsymbol{PN_c^i}$ (39)

which is the product of the probability of the particle being collected (*p*) and the number of possible particle collisions (N_c^i) (wiki/Froth_flotation)

$\boldsymbol{d_p}$ is particle diameter, $\boldsymbol{d_b}$ is bubble diameter, ***H*** is a specified height within the flotation , which the recovery was calculated, ***c*** is the particle concentration

Other following additional mathematical parameters in equations (40 to 45) were also used to evaluate the effectiveness of froth flotation processes (Kawatra, 2015)

$$\frac{F}{C} = \frac{c-t}{f-t} \quad (40)$$

Percent of metal recovered (X_R) in wt%

$$X_R = 100\left(\frac{c}{f}\right)\left(\frac{f-t}{c-t}\right) \quad (41)$$

Percent of metal lost (X_L) in wt%

$$X_L = 100 - X_R \quad (42)$$

Percent of weight recovered (X_W) in wt%

$$X_W = 100\left(\frac{C}{F}\right) = 100\left(\frac{f-t}{c-t}\right) \quad (43)$$

F is the weight percent of feed, *C* is the weight percent concentrate, *T* is the weight percent of tailings, *c*, *t*, and *f* are the metallurgical assays of the concentrate, tailings, and feed, respectively.

Ratio of feed weight to concentrate weight $\frac{F}{C}$ (unitless) (wiki/Metallurgical_assay)

When the dried froth and tailings are subjected to proximate analysis, the data obtained were used to calculate:

Combustible recovery (Eq. (44) (Taggart, 1945) ,

$$\text{Combustible recovery} = \frac{C(100-c)}{F(100-f)} x100\% \quad (44)$$

And the entrained water recovery (Eq.45) (Xia, 2016),

$$\text{Entrained water recovery} = \frac{W_c}{W_f} x100\% \quad (45)$$

where 'C' is the weight percentage of the concentrate, 'F' is the weight percentage of the feed, 'c' is the ash percentage of the froth, 'f'' is the ash percentage of the feed, 'W_c' is the weight percentage of water recovered in the froth, 'W_f' is the weight percentage of water in the pulp.

Design drawings

The drawings that emanated from the design and used for the fabrication are illustrated in Figures (4) to (13).

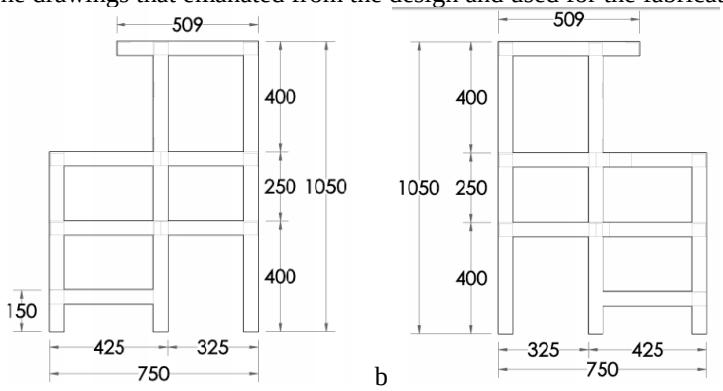

Figure 4: Right and left views (a,b) of flotation cell housing framework with dimensions (mm)

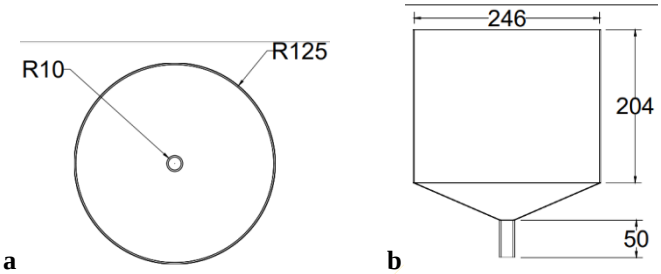

Figure 5: Plan and side views (a,b) with configuration (mm) of the mixing chamber

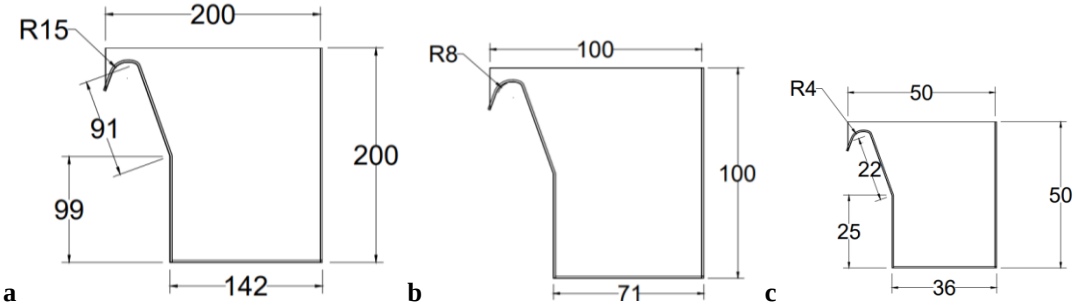

Figure 6: Side views (a-c) with configurations (mm) of the three sets of flotation baths

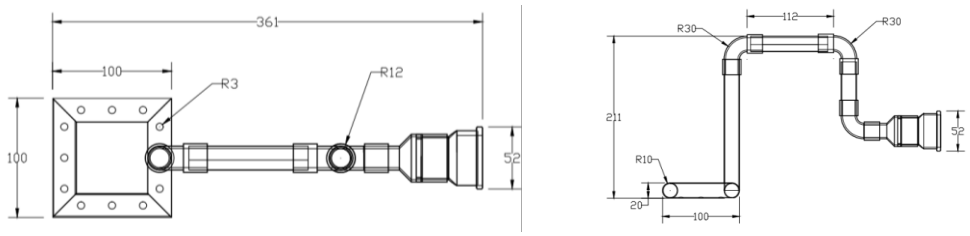

Figure 7: Plan and side views (a,b) of pipe and connectors the dimension (mm)

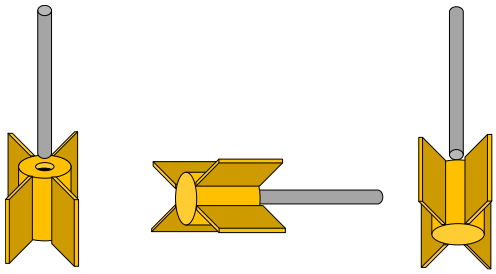
Figure 8: 3D views of impeller with shaft rod

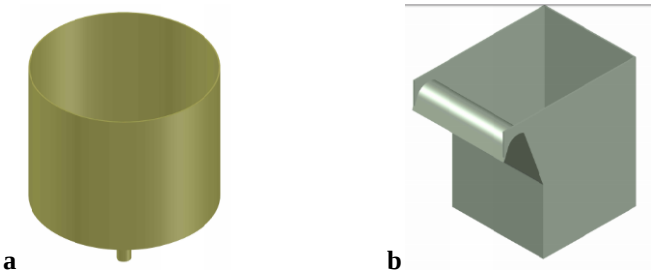

Figure 9: 3D views of the (a) mixing chamber and (b) froth flotation bath

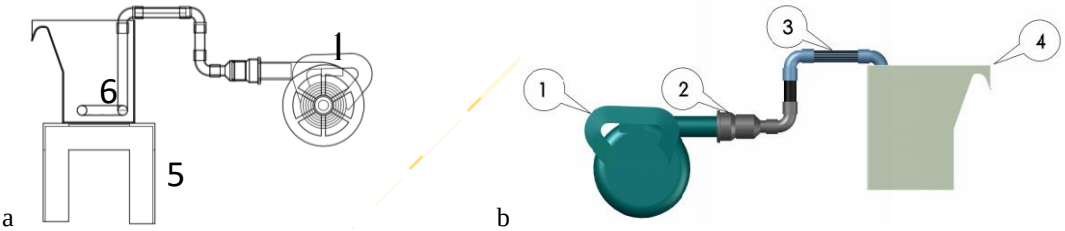

1- air blower, 2 -pipe connectors, 3-rubber pipe, and 4- flotation bath, 5-stand, 6-air outlet

Figure 10: showing 2D and 3D of pipes connectors, flotation bath, blower and stand

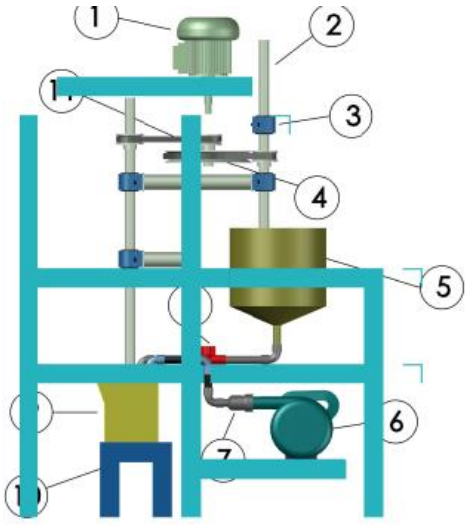

1-electric motor, 2- shaft, 3- pillow bearing, 4- pulley, 5- mixer, 6- air blower, 7- plastic pipe connector, 8- valve, 9- flotation cell, 10- bath stand, 11- belt

Figure 11: showing 3D view of the assembly of flotation set up

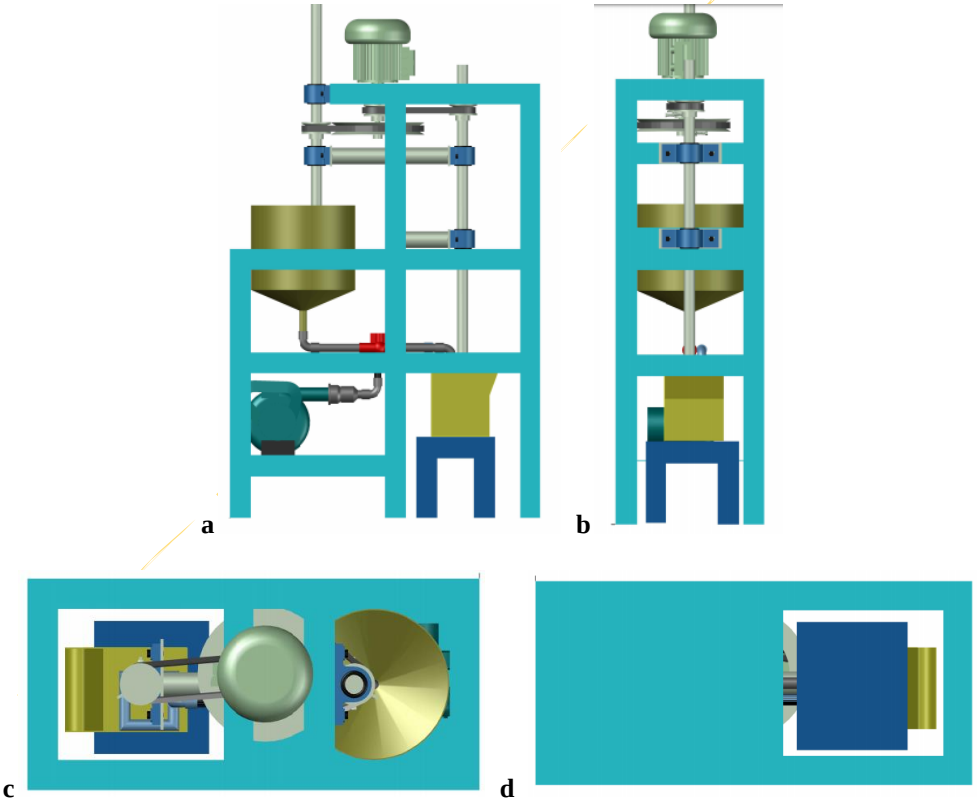

Figure 12: 3D of (a) right, (b) back, (c) plan and (d) bottom views of flotation machine

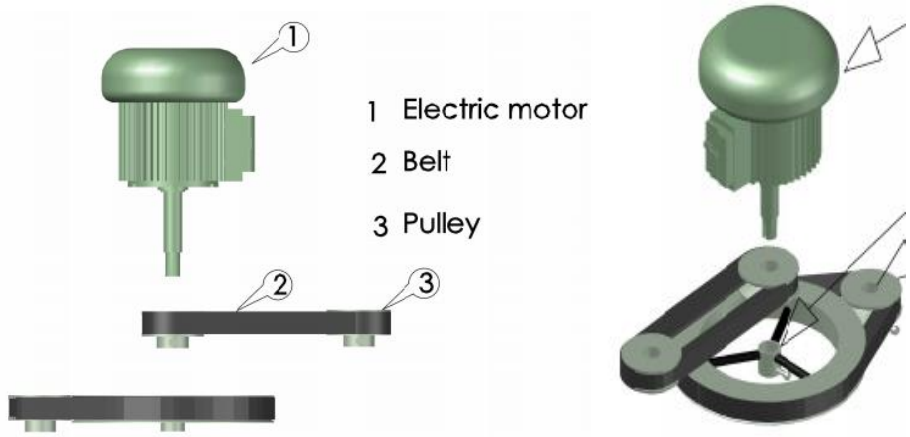

Figure 13: 3D views of de-assemble of electric motor, small and big pulleys, and belts

Materials selection

Table 2: Materials selection table for components

Machine components	Material/ specifications	Qty	Selection reasons
Reagent-pulp mixing chamber	1.5 mm thick stainless steel plate	1	It is corrosion resistance and because of its flexibility to be formed into required shape. Container for mixing reagents and the mineral pulp to be separated and mix it before passing it down to the bath for separation.
Floatation bath/cell	1.5 mm thick stainless steel plate	3 set	It is corrosion resistance and because of its flexibility to be formed into required shape. The troughs for separation of mineral.
Framework	5.08 mm thick angle mild steel bars	1	High rigidity and weldability
Prime shaft rods		1	
Impeller shaft rods		2	
Pulleys		5	This positioned the belt and rotates the shafts
V- belt	Rubber fiber	2	High resistance to heat and chemical substance.
Electric motor	0.5 hp	1	Low speed which will be very suitable for the required rotary force needed in the bath. The AC electric motor rotates the pulleys / shafts / impeller to agitate the bath.
Impellers	High chromium steel rods	2	High corrosion resistance. This is the part of the machine which rotates and produces slurry to the solution of minerals and floatation reagents.
Pipes	Plastic (PVC)	1	Corrosion resistant, economical and suitable for fluid movement. Conveys the mineral pulp and/with reagents to the floatation bath.
Air hose			Supplies air from the blower to the flotation bath
Bolt and nut	Mild steel (Ø20 mm)	12	Rigidity property, easy tightening and loosening.
Blower	Plastic cover	1	Very light and efficient. Supplies air into the floatation bath through the linking with pipe.

Table 3: Design calculations and parameters

Parts of Machine	Value	Units
Volume of Mixing chamber (V)	10836.8	cm^3
Cylindrical Part of Mixer	10018.3	cm^3
Conical Part of the mixer	818.49	cm^3
Power required	0.5/1.119	hp/kw

Volume of flotation bath	3920	cm^3

Table 4: Cost of production

Material	Specifications of Materials	Quantity	Unit Cost (₦)	Total Cost (₦)
Ball bearing	diameter, 20 mm	4	5,000	20,000
Chromium rod	diameter, 20 mm	160 cm	12,000	12,000
Belt	rubber fiber	2	1500	3,000
Pulley (small)	diameter, 50 mm	3	2500	7,500
Pulley (big)	diameter, 165 mm	1	4,500	4,500
Angle steel bar	50 mm x 4 mm x 5mm	3	8,000	24,000
Stainless plate	2440 mm x 1220 mm	1	35,000	35,000
Electric motor	0.5 hp (0.373kw)	1	23,000	23,000
Blower	0.5 hp(0.373kw)	1	8,000	8,000
Bolts & nuts	diameter, 20 mm	12	150	1,800
Paint	Gloss	4 ltrs	1,750	7,000
Painting				5,000
Plastic pipes, connectors				5,550
Consumables				15,500
Skilled labour				25,000
Machining and connector				4000
Electrification				4000
Rolling and Folding				1000
Logistics				7,500
Consultations				10,000
			Total	223,350

Fabrication and assembly of components

From the various data obtained from the designed calculations of components, specifications and configurations for the frames, flotation bath, impeller and the mixer were analyzed and evaluated. Welding was adopted for the joining of frames of the froth floatation and the floatation bath using electric arc method for the large flexibility of managing the controlling parameters such as the thickness of the material being welded and the shape of joining metal.

The design takes into account the regular inspection of the weld joints on its completion, while threaded bolts and nuts as fasteners provide the clamping force holding the pillow bearing with the frame of the machine.

The safety procedures were observed in the design and fabrication of the froth flotation machine as well as during its operation. The frame rigidity/firmness is fundamental to avoid vibrations and dangling during the operation process. The electric motors and air blower were fixed into the framework by bolts and nuts. The electric motor transmits energy to the two suspended rotating impellers via the long shafts, pulleys and belts. The mixer was design to be relatively large volume to ensure continuity of feed inflow to the flotation cell and avoid spillage of the concentrate on the ground floor during operation. For the reason of fluid flow control, a valve was incorporated along the pipeline carrying the pulp from the mixer to the bath. The blower is installed close to the floatation bath whereby the air is easily transferred into the flotation cell.

.

RESULTS AND DISCUSSIONS

Test running the machine

The fabricated structure (Figure 14, 15) was test run to examine and assess the performance of the machine and its operation. The efficiency of the electric motor was tested to check the speed of the turning rod which will be exerted on the impeller during operation of the machine. The efficiency of the electric blower is also checked to ascertain the actual air flow rate and pressure that will be needed for the floatation process

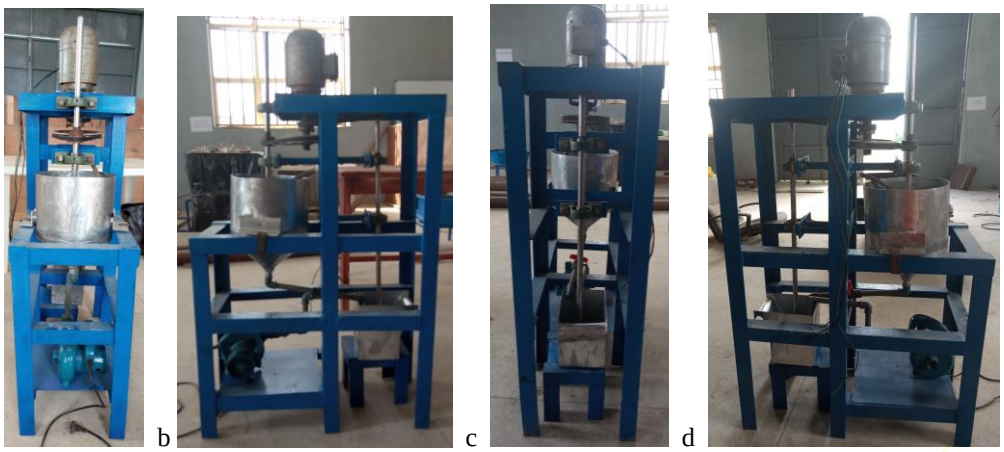

Figure 14: Photographs of a- front view, b- right side view, C - back view and, d-'left side view of flotation machine

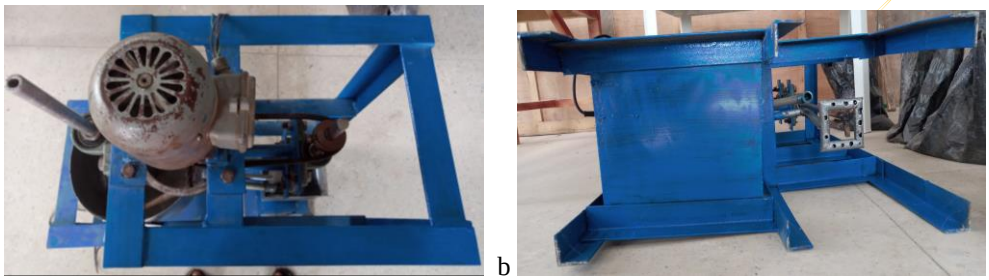

Figure 15: Photographs of a- aerial plan and, b- bottom views of flotation machine

Preparing materials for flotation

The materials preparation for the flotation process entails crushing, grinding and mixing into the proportionate. The mineral to be floated is determined with the consideration of its affinity to air.

Maintenance of machine and safety

The following maintenance tasks are to be observed regularly in the cause of the usage and the operation of the blower:

Chemical cleaning: Water treatment is necessary to aid in the removal of oxygen in the feed water and prevents corrosion. The chemical cleaning process of froth flotation machine removes pollutant and impurities that impedes the transfer of heat within the generator that may result in system failure. Hot alkaline chemical cleaning can be used to remove oil, grease, and other protective coating that were unnecessary during the fabrication of the froth flotation machine but will act as pollutant and impurities during operation.

Flushing with water: This simply involves washing of the mixer and baths after carrying any experiment to cleanse out the trap particles inside pipes.

General cleaning of the machine is vital to make it dirt free.

Periodic examination and lubrication of mating parts such the pillow is important.

CONCLUSION AND RECOMMENDATIONS

The floatation machine has been designed, fabricated and constructed based theoretical principles of flotation design and calculations. The materials selection considered the cost and availability of the materials. The experimental tests carried out on the floatation machine show that it is efficient, simple to maintain, economical to produce and install. The machine is simple enough to be reproduced based on the design specifications already highlighted in this discuss.

However, there areas in which further research focuses have to be given include: the comparative studies on types of impeller that best suit the froth recovery of mineral in the fabricated machine; the determination of the inclination angle of the impeller blades for optimum agitation efficiency, the need to engage better speed reducing mechanism different from the pulley system as to enhance optimum froth stability and longer mineral-air engagement time; as well as possibility of scaling up and upgrading the machine by automation.

REFERENCES

Aghazadeh S., Mousavinezhad S.K., Gharabaghi M., (2015) Chemical and colloidal aspects of collectorless flotation behavior of sulfide and non-sulfide minerals, Adv. Colloid Interface. 225 (2015) 203–217.

Ajibola O.O, Adebayo A.O, Akipeloye S,, Oladimeji V., Oyekanmi A., Ogungbe G., Omoyeni D.O, Borisade S.G, Oloruntoba D.T and Adewuyi B.O. (2021). Fabrication and performance evaluation of electroless-nickel deposition line for metal alloys and plastic substrates. FUW Trends in Science & Technology Journal, Vol. 6 No. 1 pp. 069 – 078

Ajibola O.O, Alamuoye O.F, Omoyeni D.O., Adebayo A.O., Borisade S.G., Olotu V., Adetoye O., Adebanji S. (2020) Design and fabrication of a multi-purpose homogenizer, NIPES Journal of Science and Technology Research 2(3) 2020 pp. 21-35

Aldrich C., Marais C., Shean B.J., Cilliers J.J., (2010) Online monitoring and control of froth flotation systems with machine vision: A review. International Journal of Mineral Processing 96 (2010) 1–13

Allen, G. (1995). Bubble mechanism. Institute of Metallurgy. UK

Angadi S.I., Jeon H., Nikkam S. (2012) Experimental analysis of solids and water flow to the coal flotation froths, International Journal of Mineral Processing 110–111 (2012) 62–70

Angadi S.I., Suresh N., (2005) A kinetic model for the prediction of water reporting to the froth products in batch flotation, Miner. Process. Extr. Metall. 114 225–232.

Anzoom S.J., Tripathy S.K., Sahu L., Bhattacharya S., Mukherjee A.K., (2020) Influence of impeller speed and cell volume on coal flotation performance in a self-aerating flotation machine Advanced Powder Technology 31 (2020) 4053–4063.

Arbiter N., Harris C., (1979) Design and operating characteristics for large flotation cells, SME Inc Littleton CO USA (1979) 8.

Bergh, L., Yianatos, J., (2011). The long way toward multivariate predictive control of flotation processes. J. Process Control 21, 226–234.

Crane Engineering-Cleveland Mixer, -The plant engineer's guide to mixing and agitation Design and Fundamentals Manual (P33). Retrieved on 31-05-2-21:22:42

Dairo O.U. Olayanju T.M, Adeoye A.A., Adeleke A.E., Adeosun O.J. and Iyerimah R.B., Development of an anaerobic digester for animal waste, FUOYE Journal of Engineering and Technology, 2017, Volume 2, Issue 2, pp 17-22

Deglon, D., (2005). The effect of agitation on the flotation of platinum ores. Miner. Eng. 18, 839–844.

Degner, V. R. (1988). Column Flotation '88 - Proceedings of an international Symposium. In K. S. K., Flotation Fundamentals (pp. 267-280). Leeds.

Dibrov I.A., Voronin N.N., Klemyatov A.A., (1998) Froth floto-extraction, a new method of metal separation from aqueous solutions, Int. J. Miner. Process. 54 (1) (1998) 45–58.

Eberts, D. H. (1986). Flotation-Choose the Right Equipment for your Needs. Canadian Mining Journal, 25-33.

Erameh Andrew A, Adingwupu Anthony C, Design and Development of a Hand Operated Grinding Machine. Advances in Engineering Design Technology. Vol. 1 No.1, pp. 49-64

Erik, O.; Franklin, D. J.; Brook, I. H. and Henry, H. R. (2004). Machinery handbook. Industrial press inc., New York, USA

Ferreira, J.P., Loveday, B.K., (2000). Improved model for simulation of flotation circuits. Miner. Eng. https://doi.org/10.1016/S0892-6875(00)00129-1.

Froth_Flotation (2019). Available at Wikipedia: ttp://en.m.wikipedia.org/wiki/Froth_flotation, Retrieved on 04-05-2019-21:15

Gorain B. K., (2000). Flotation Cell Design: Application of fundamental principles. In Flotation (p. 1502). Academic Press. Queensland

Harris C., Lepetic V., (1966) Flotation cell design, Min. Eng. 18 (1966) 67–72.

Holtham, P., Nguyen, K., (2002). On-line analysis of froth surface in coal and mineral flotation using JKFroth Cam. Int. J. Miner. Process. 64, 163–180.

https://en.wikipedia.org/wiki/Froth_flotation#Science_of_flotation

https://en.wikipedia.org/wiki/Metallurgical_assay

Jahedsaravani A., Massinaei M., Marhaban M.H., (2017) Development of a machine vision system for real-time monitoring and control of batch flotation process, International Journal of Mineral Processing 167 (2017) 16–26

Jameson G.J., Cooper L., Tang K. K., Emer C., (2020) Flotation of coarse coal particles in a fluidized bed: The effect of clusters. Minerals Engineering 146 (2020) 106099

Jameson, G.J., (2010a). New directions in flotation machine design. Miner. Eng. 23 (11–13), 835–841.

Jameson, G.J., (2010b). Advances in fine and coarse particle flotation. Canad. Metall.Quart. 49 (4), 325–330.
Jovanović, I., Miljanović, I., (2015). Contemporary advanced control techniques for flotation plants with mechanical flotation cells–a review. Miner. Eng. 70, 228–249.
Jovanović, I.,Miljanović, I., Jovanović, T., (2015). Soft computing-based modeling of flotation processes–a review. Miner. Eng. 84, 34–63.
Kaartinen J., Hätönen J., Roine T. Machine Vision of Flotation Froths with a Rapid-Prototyping Platform, IFACMMM (2009). Viña del Mar, Chile, 14 -16 October 2009
Kaya M., (2005) The use of froth flotation in environment protection, France.
Khurmi, R.S. and Gupta, J.K. (2005). Machine Design. Eurasia publishing house (PVT) Ltd. Nagar, New Delhi.
Kawatra, S. K. (2015). Floatation Fundamentals, MTU. Available at http://www.chem.mtu.edu/chem_eng/faculty/kawatra/Flotation_Fundamentals.pdf
Kawatra, S.K (1987). Column Flotation of Coal; In M. a. Eds, Fine Coal Processing Noyes Publication. Park Ridge, pp. 414-429.
Laskowski, J.S., (2001). Coal Flotation and Fine Coal Utilization, Volume 14, 1st Edition Elsevier Science.
Li C., Runge K., Shi F., Farrokhpay S. (2018) Effect of froth rheology on froth and flotation performance, Minerals Engineering 115 (2018) 4–12
Li C., Wang L.. (2018) Improved froth zone and collection zone recoveries of fine mineral particles in a flotation column with oscillatory air supply Separation and Purification Technology 193 (2018) 311–316
Li F., Zhong H., Xu H., Jia H., Liu G., (2015) Flotation behavior and adsorption mechanism of α-hydroxyoctyl phosphinic acid to malachite, Miner. Eng. 71 (2015) 188–193.
Li Z., Fu Y., Li Z., Nan N., Zhu Y., Li Y., (2019) Froth flotation giant surfactants. Polymer 162 (2019) 58–62
Liu S., Ge Y., Fang J., Yu J., Gao Q., (2020) An investigation of froth stability in reverse flotation of collophane. Minerals Engineering 155 (2020) 106446
Maldonado, M., Desbiens, A., Del Villar, R., Quispe, R., (2007a). Towards the optimization of flotation columns using predictive control. IFAC Proc. Vol. (IFAC-PapersOnline) 12, 75–80. https://doi.org/10.3182/20070821-3-CA-2919.00011.
Maldonado, M., Sbarbaro, D., Lizama, E., (2007b). Optimal control of a rougher flotation process based on dynamic programming. Miner. Eng. 20, 221–232. https://doi.org/10.1016/j.mineng.2006.08.015.
Mathe, Z., Harris, M., O'Connor, C., (2000). A review of methods to model the froth phase in non-steady state flotation systems. Minerals Engineering 13 (2), 127–140.
Mesa D., Morrison A.J., Brito-Parada P.R., (2020) The effect of impeller-stator design on bubble size: Implications for froth stability and flotation performance, Minerals Engineering 157 (2020) 106533
Mesa, D., Brito-Parada, P.R., (2019). Scale-up in froth flotation: a state-of-the-art review. Sep. Purif. Technol. 210, 950–962.
Michuad, L. D. (2016). Flotation Cell, Available on 911 Metallurgist: https://www.911metallurgist.com/blog/floataion-cell. Retrieved on 20-04-2016
Nelson, M. (2012). From 10 Cubic Feet to 500 Cubic Meters-- Observation on 100 Years of Flotation Technology" In Separation technologies, Edited by Courtney Young et al. Society of Mining, Metallurgical and Exploration. pp 539-546.
Nunez F., Tejeda G., Silva D., Cipriano A. Global (2009) Characterization of Froth Speed Behavior in a Rougher Flotation Line, IFACMMM 2009. Viña del Mar, Chile, 14 -16 October 2009
Osarenmwinda J.O and Iguodala K.O (2014); Design and fabrication of a foundry sand mixer using locally avaliable materials. Nigerian Journal of Technology (NIJOTECH) Vol. 33 No. 4, pp.604-609
Quintanilla P., Neethling S. J., Brito-Parada P. R., (2021) Modelling for froth flotation control: A review. Minerals Engineering 162 (2021) 106718
Rubinstein, J. B. (1995). Column Floataion Processes. Gordon and Breach Basel. Switzerland, p300 .
Saravani, A., Mehrshad, N., Massinaei, M., (2014). Fuzzy-based modeling and control of an industrial flotation column. Chem. Eng. Commun. 201, 896–908.
Schulze, H. J. and Nguyen A. V. (2004), Colloidal Science of Flotation: In Surfacant Science Series, vol. 118; Marcel Dekker, New York
Shean, B., Cilliers, J., (2011). A review of froth flotation control. Int. J. Miner. Process. 100, 57–71.
Smieszek, Z. (2001). Floataion machine for mining industry. Institute of Non-Ferrous Metals. Poland
Somasundaran P., Kunjappu J.T., (1989) In-situ investigation of adsorbed surfactants and

polymers on solids in solution, Colloids Surf., A 37 (1989) 245–268.
Tabosa, E., Runge, K., Holtham, P., (2016). The effect of cell hydrodynamics on flotation performance. Int. J. Miner. Process. 156, 99–107.
Taggart A.F. (1945) Handbook of Mineral Dressing, Wiley, 1945.
Trahar, W.J., (1981). A rational interpretation of the role of particle size in flotation. Int. J. Miner. Process. 8, 289–327.
Warren, L.J., (1985). Determination of the contribution of true flotation and entrainment in batch flotation tests, Int. J. Miner. Process. 14, 33–44.
Xia W., Xie ., G., Peng Y., (2016) Comparison of flotation performances of intruded and conventional coals in the absence of collectors, Fuel 164 (2016) 186–190.
Yianatos J., Bergh L., Tello K., Díaz F., Villanueva A. (2008) Froth mean residence time measurement in industrial flotation cells Minerals Engineering 21 (2008) 982–988
Yoon, R.H., Luttrell, G.H., Adel, G.T., Mankosa, M.J., (1992). The application of Microcel™ column flotation to fine coal cleaning. Coal Preparation 10, 177–188.
Zarie M., Jahedsaravani A., Massinaei M., (2020) Flotation froth image classification using convolutional neural networks. Minerals Engineering 155 (2020) 106443